Machine Learning and hybrid models for assessing climate change impacts on runoff in the Kasilian catchment, Northern Iran
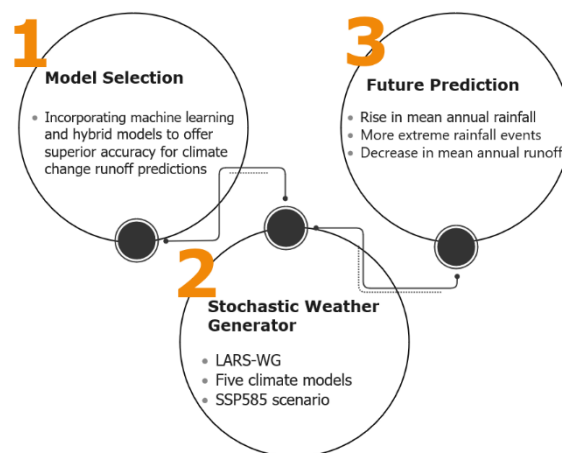
Farhad Hajian[1,*] iD, Hossein Monshizadeh Naeen[2] iD

[1]Department of Civil Engineering, Neyshabur Branch, Islamic Azad University, Neyshabur, Iran.
[2]Department of Computer Engineering, Neyshabur Branch, Islamic Azad University, Neyshabur, Iran.

GRAPHICAL ABSTRACT

ARTICLE INFO

ABSTRACT

This study evaluates the performance of Artificial Neural Networks (ANNs), Gene Expression Programming (GEP), and the HEC-HMS models in assessing the impacts of climate change on runoff in the Kasilian catchment, northern Iran. Daily data from 2007 to 2021 were divided into calibration (2007–2018) and validation (2018–2021) periods. The results indicate that GEP and ANN models surpassed the HEC-HMS model across all performance metrics, including RMSE and NSE, when applied individually. Furthermore, hybrid models, integrating HEC-HMS with GEP and HEC-HMS with ANN, exhibited superior performance compared to individual machine learning (ML) or HEC-HMS models. Input variables (temperature and rainfall) were generated using LARS-WG software, incorporating five climate models and the SSP585 scenario for future climate change studies. Additionally, these hybrid models were used to forecast runoff changes for the observed period (2007-2018) and future periods (2031-2050 and 2051-2070). The results show a rise in average annual precipitation, extreme precipitation events, and precipitation intensity, implying a higher likelihood of flooding and erosion in the future for the Kasilian Catchment and similar small catchments in north of Iran.

1. Introduction

Accurately predicting runoff by considering rainfall, evaporation, and other hydrological factors is a vital aspect of water resources engineering. Recently, Artificial Neural Networks (ANNs) and Genetic Programming (GP) have gained significant popularity in this domain

(Kisi, Shiri, and Tombul, 2013). Valipour *et al.* (2013) employed Auto-Regressive Integrated Moving Average (ARIMA), autoregressive moving-average (ARMA), and artificial neural network (ANN) techniques to forecast the inflow of the Dez Dam reservoir in Iran. They utilized monthly flow data from 1960 to 2007, with 42 years allocated for training and 5 years for testing. Their results revealed that an ANN

*Corresponding author Email: f.hajian@yahoo.com

with a sigmoid activation function and 17 neurons in the hidden layer was the most effective model for predicting the inflow. In another study, researchers allocated 70% of the dataset for training purposes and the remaining 30% for testing. They applied an artificial neural network to data spanning from 1951 to 2006, covering fifty-five years. The evaluation revealed that the multilayer perceptron neural network outperformed the radial basis function. The study highlighted that both the two-day antecedent rainfall and the one-day antecedent discharge had a significant impact on runoff. The mean squared error values were 0.8 for the training data and 0.75 for the testing data (Motamednia et al., 2015). In another research, Pashazadeh et al. (2020) compared three models of GEP, ANN, and Muskingum in predicting the outlet hydrograph in the floodway of Qarasu River. The GEP model has demonstrated superior performance in estimating the outlet hydrograph of river flow when compared to the Muskingum and ANN models. Chavoshi et al. (2013) applied artificial neural networks (ANNs) to predict flood events in the southern Caspian Sea catchment. They compared the results from the ANN model with those from a multiple regression model and found that the ANN model handled the complexity of hydrological problems more effectively. Among the various ANN architectures evaluated, the multilayer feed-forward backpropagation network using the Levenberg–Marquardt algorithm demonstrated the best performance. Aytek, Asce, and Alp (2008) compared artificial neural networks (ANNs) and evolutionary computation (EC) for modeling rainfall and runoff interactions. Aytek, Asce, and Alp (2008) discovered that evolutionary models, such as GEP and GP, performed better than ANN methods, including feed-forward back-propagation (FFBP) and generalized regression neural network (GRNN). Wang et al. (2009) assessed several models for predicting monthly discharge time series. The study evaluated several models, including ARMA models, ANN, adaptive neural-based fuzzy inference systems (ANFIS), GP, and support vector machines (SVM). Their results demonstrated that the GP, ANFIS, and SVM models provided the most accurate forecasts. Azamathulla et al. (2011) investigated different modeling approaches for the stage-discharge relationship in the Pahang River. They evaluated ANN, GP, and GEP. Notably, the GEP model surpassed both ANN and GP, along with traditional models, in performance. Shiri et al. (2012) examined the effectiveness of three models— GEP, ANFIS, ANN —for forecasting daily streamflow. The study found that the GEP model significantly outperformed both the ANN and ANFIS models. Kisi, Shiri, and Tombul (2013) explored the modeling of rainfall-runoff processes using three distinct methods: ANNs, ANFIS, and GEP. Their research demonstrated that Gene Expression Programming (GEP) offers a viable and effective alternative to traditional models for accurately simulating the rainfall-runoff process. The previously mentioned studies suggest that evolutionary techniques, particularly Gene Expression Programming (GEP), surpass Artificial Neural Networks (ANNs) in the simulation and prediction of hydrologic models.

Asadi and Santos (2022) developed a hybrid model by coupling HEC-HMS output with ANN for simulating daily discharge in the Kallada River basin, Kerala, India. The hybrid model showed better performance in simulating daily discharge and estimating yearly peak discharge compared to the individual HEC-HMS and ANN models. Gebremichael and Hailu (2024) evaluated the efficacy of HEC-HMS, ANN, and SVR models in predicting runoff in the upper Baro catchment, Ethiopia. The study found that while ANN outperformed HEC-HMS, integrating the outputs from HEC-HMS into machine learning models could potentially enhance prediction accuracy.

Conceptual models, such as HEC-HMS, have been valuable for runoff estimation. However, they face challenges related to non-uniqueness of parameter values and reliance on indirect data sources. Estimating these parameters, especially soil physics and vegetation physiology, can be difficult. Additionally, compensation effects between model parameters exist (Hajian, 2013). Furthermore, limited research has explored the use of Artificial Neural Networks (ANN) and Gene Expression Programming (GEP) in studying the effects of climate change on water resources. This area of research demands more attention, particularly due to the scarcity of field data. The current study aims to evaluate the accuracy of three models—Gene Expression Programming (GEP), Artificial Neural Network (ANN), and HEC-HMS—in modeling rainfall-runoff processes. Additionally, it examines the impact of climate change on runoff in the Kasilian Catchment, emphasizing the models that exhibited superior performance.

2.material and methods
2.1. Study area

This study centers on the Kasilian Catchment located in Mazandaran Province, northern Iran, spanning from 53°18′ to 53°30′E and 35°58′ to 36°07′N (Fig. 1). The catchment area, which extends over 65.7 km² upstream of the Valikbon hydrometric station, flows northward into the Caspian Sea. The catchment's longest flow path extends for 17.8 kilometers. Around 80% of the catchment area is covered by forests, while the downstream areas have been cleared for agricultural use. The geological composition includes shale, sandstone, marl, and siltstone. Daily rainfall and temperature data are recorded at the Sangdeh meteorological station, and river discharge is monitored at the Valikbon station (Fig. 1). Between 1977 and 1996, the average annual rainfall was around 756 mm, and from 1980 to 1996, the average annual runoff was 229 mm (Hajian, 2013).

2.2. HEC-HMS modeling of rainfall-runoff process

HEC-HMS, created by the US Corps of Engineers, is extensively utilized for hydrological studies worldwide. This research employed the Thornthwaite method to calculate potential evapotranspiration (PET) for the HEC-HMS, ANN, and GEP models (see Table 1), given that only temperature data is available for the Kasilian Catchment. Despite this limitation, in climate change studies, uncertainties in PET have a lesser impact on simulated runoff than those stemming from different GCM types or projected future climate scenarios (Bae et al., 2011, Hajian, 2013).
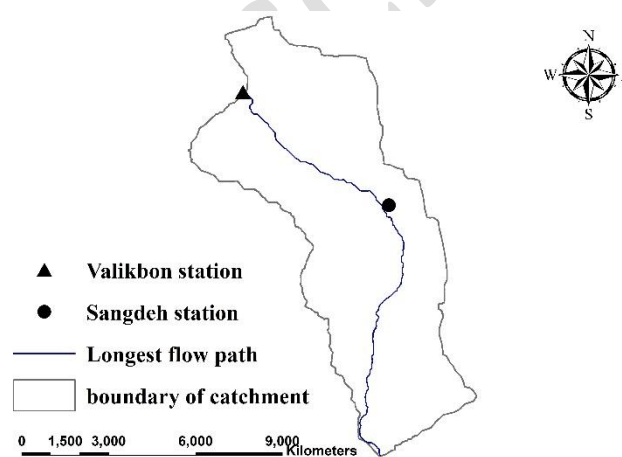

Fig. 1. Outline map of the Kasilian Catchment.

HEC-HMS requires 23 parameters to model hydrological dynamics within a catchment. Initial estimates for these parameters are refined through automated optimization using the Nelder-Mead method, aiming to minimize the difference between observed and computed runoff volumes (Scharffenberg and Fleming, 2010). In this research, primary parameter values were sourced from geology, soil, and land use maps, along with data from existing literature (Hajian, 2013). A conventional calibration-validation process was employed, where parameter optimization occurred during the calibration stage. For the calibration period (September 23, 2007, to March 20, 2018), the Nash and Sutcliffe coefficient was -0.293, while for the validation period (September 23, 2018, to September 22, 2021), it was 0.060. Additionally, the RMSE coefficient during calibration was 0.625, and during validation, it was 0.870. This poor result is due to seasonal variations in parameter values and the inherent uncertainty associated with these parameters. Additionally, HEC-HMS is unable to model the rainfall-runoff process seasonally.

2.3. ANN modeling of rainfall-runoff process

Human brains use over 10 billion neural cells to process information and solve problems. These neurons, though limited individually, collectively perform complex computations and pattern recognition. Neurons learn from their environment and form connections, consisting of dendrites (input), cell bodies (processing), and axons (output). Inspired by this biological structure, Artificial Neural Networks (ANNs) mimic brain neurons for tasks like classification, pattern recognition, and regression. In ANNs: 1. Inputs represent dendrites.2. Weights model synaptic spaces.3. Activation functions simulate cell body influence. 4. Outputs correspond to axons.
Hidden layers between input and output layers enable ANNs to learn and model complex patterns through multiple processing stages. Each artificial neuron is a mathematical representation involving inputs,

weights, thresholds, activation functions, and outputs (Romański *et al.*, 2017). This process can be mathematically represented as (Ömer and Ayan 2015):

$$y_i = f_i(\sum_{j=1}^n w_{ij} \times x_j + \theta_i) \tag{1}$$

where, (y_i) is the output, (w_{ij}) are the weights, and (θ_i) is the bias. ANNs excel in regression tasks by predicting continuous values and modeling complex input-output relationships, making them ideal for practical applications. Among the various ANN architectures, the feed-forward back propagation model with the Levenberg–Marquardt algorithm for optimizing the weights during the training process has demonstrated superior performance (Bakhshaei *et al.*, 2021). For many nonlinear problems, a single hidden layer is often adequate. Additionally, research indicates that incorporating more than two hidden layers does not significantly enhance performance (Pashazadeh and Javan, 2019; Bakhshaei *et al.*, 2021; Kisi, Shiri, and Tombul, 2013). The precipitation and potential evapotranspiration estimated by Thornthwaite method over catchment is computed as a main input to the ANN and GEP models.

Table 1. Different combinations of input variables for training and testing of the models

Model number	Input combination	output
1	P_t, P_{t-1}, ET_t, ET_{t-1}	Q_t
2	P_t, P_{t-1}, P_{t-2}, ET_t, ET_{t-1}, ET_{t-2}	Q_t
3	P_t, P_{t-1}, P_{t-2}, P_{t-3}, ET_t, ET_{t-1}, ET_{t-2}, ET_{t-3}	Q_t
4	P_t, P_{t-1}, P_{t-2}, P_{t-3}, P_{t-4}	Q_t

Table 2. The performance assessment of various ANN models with differing architectures.

Model number detailed in Table 1	Activation function	Number of neurons in hidden layer	NSE Train	NSE test	RMSE train	RMSE test
1	Tansig	10	0.166	-0.0015	0.5018	0.898
	Tansig	3	0.1477	-0.0025	0.5073	0.899
	Purelin	10	0.1082	-0.0021	0.519	0.899
	Purelin	3	0.119	0.0109	0.5158	0.893
2	Tansig	10	0.165	0.03	0.502	0.896
	Tansig	3	0.181	0.039	0.497	0.88
	Purelin	10	0.130	0.054	0.512	0.873
	Purelin	3	0.139	0.019	0.509	0.889
3	Tansig	10	0.078	-0.078	0.527	0.932
	Tansig	3	0.084	-0.0019	0.526	0.899
	Purelin	10	0.152	0.502	0.505	0.874
	Purelin	3	0.15	0.028	0.506	0.885
4	Tansig	10	0.187	-0.031	0.495	0.912
	Tansig	3	0.176	0.034	0.498	0.882
	Purelin	10	0.231	0.065	0.481	0.868
	Purelin	3	0.188	0.048	0.495	0.876

The ANN model used in this study comprises three neuron layers: an input layer, a hidden layer, and an output layer. In this study, we enhanced the ANN's performance by normalizing the input data during preprocessing. We employed the min-max method to scale the data to a specific range, typically [0, 1], which accelerates the training process and improves model performance. To improve the overall performance of the artificial neural network (ANN) model for this particular application, a sensitivity analysis was conducted. This analysis involved exploring various ANN structures, including different network types, training functions, hidden layer neuron counts, and transfer functions. Table 2 presents the performance evaluation of various ANN models using the NSE and RMSE statistical indices.

2.4. GEP modeling of rainfall-runoff process

Gene Expression Programming (GEP) is a type of algorithm that creates models by copying how evolution and natural selection work. In GEP, computer programs are shown as tree-like structures that can change and improve over time. These programs are stored in fixed-length sequences, called chromosomes, which act like a blueprint (genotype). The tree structures that result from these sequences are called expression trees and represent the actual solution (phenotype). This setup helps GEP to find and refine solutions to different problems by changing the size, shape, and content of the expression trees

(Ferreira, 2006). In GEP modeling, selecting an appropriate fitness function is the initial step (Kisi, Shiri, and Tombul, 2013). Various default functions from GeneXpro, including addition, subtraction, multiplication, division, power, square root, exponential, natural logarithm, absolute value, inverse, cube root, sine, cosine, tangent, cotangent, arcsine, arccosine, arctangent, and additional linking functions, were utilized to build the GEP models. Table 3 presents the performance evaluation of different GEP models using the NSE (Nash-Sutcliffe Efficiency) and RMSE (Root Mean Square Error) statistical indices.

2.5. Hybrid modelling approach (Integrating machine learning (ML) with conceptual models)

Integrating conceptual models with machine learning (ML) techniques, such as artificial neural networks (ANN) or gene expression programming (GEP), enhances runoff prediction accuracy. Utilizing the streamflow estimates from the conceptual model as inputs for machine learning models like ANN and GEP will enhance the accuracy of the forecasted runoff. Studies, such as those by Farfan *et al.* (2020) and Hitokoto and Sakuraba (2020), have demonstrated the effectiveness of this method, resulting in markedly improved streamflow predictions. These examples highlight the potential of combining conceptual and ML models for more accurate and reliable runoff predictions.

Table 3. The performance evaluation of different GEP models

Model number detailed in Table 1	NSE Train	NSE Test	RMSE Train	RMSE Test
1	0.101	0.022	0.521	0.888
2	0.143	0.020	0.508	0.889
3	0.078	-0.019	0.527	0.906
4	0.223	0.031	0.484	0.883

Table 4. The performance evaluation of different hybrid models.

	Integration HEC HMS & GEP (*)				Integration HEC HMS & ANN (3,3,1) with tansig activation function			
	NSE	NSE	RMSE	RMSE	NSE	NSE	RMSE	RMSE
Hybrid	train	test	train	test	train	test	train	test
model	0.291	0.133	0.243	0.836	0.274	0.163	0.476	0.821

The performance of the ANN model, integrated with the calibrated HEC-HMS model from section 2.2, was tested using hidden layers with 3 and 10 neurons, evaluating two activation functions: purelin and tansig. The results indicate that the tansig activation function with 3 neurons in the hidden layer provides better model performance. Because of space limitations, the paper does not include the results of other configurations, such as different activation functions and varying numbers of hidden layer neurons (see Table 4). The inputs to the ANN model include discharge estimates from HEC-HMS (Q_t), as well as these estimates with one lag (Q_{t-1}) and two lags (Q_{t-2}), representing the discharge from previous days. According to Table 4, integrating Artificial Neural Networks (ANN) and HEC-HMS, as well as Genetic Programming (GEP) and HEC-HMS, outperformed using Machine Learning (ML) or HEC-HMS alone. The best performance was achieved by a single hidden layer neural network using the tansig activation function and the Levenberg–Marquardt learning algorithm. For climate change investigations, the optimal ANN architecture was identified as ANN (3,3,1), which includes 3 input neurons, 3 hidden layer neurons, and 1 output neuron.

Integrating HEC-HMS with Gene Expression Programming (GEP) offers an advantage: GEP can provide a clear mathematical relationship between input and output variables, a feature not present in ANN and ANFIS models (Kisi, Shiri, and Tombul, 2013). The corresponding GEP expression for Model (*) in Table 4 is:

$$Y = \mathrm{acot}(\cos\left(\sqrt[3]{((G1C0 \times d[2]) \times G1C1)^{tanG1C4}}\right) +$$
$$\sqrt[3]{1 - \sqrt[3]{((G2C1 - d[0]) + G2C8 + (d[2] - d[0]))}} +$$
$$\mathrm{arctan}(\arctan(\arctan(\arctan(\arctan(\arctan(\sin(G3C2)))))))) \quad (2)$$

G1C1 = -2.85716229743339; G1C4 = 6.87689168980987; G1C0 = -0.19608447523423; G2C8 = 3.11519563621235; G2C1 = 0.787598787273076; G3C2 = -9.69426648762474; d [0] = discharge estimates from HEC-HMS (Q_t), d [2] = discharge estimates from two days earlier (Q_{t-2}).

Genetic operators for the highest-performing model, Model * from Table 4, are as follows: chromosome count: 30, head size: 8, gene count: 3, linking function: addition, fitness function: RMSE, Mutation rate: 0.00138, inversion rate: 0.00546.

The sensitivity analysis in the GEP model indicated that the model is highly sensitive to d0 and, to a lesser extent, to d2 (Fig. 2).
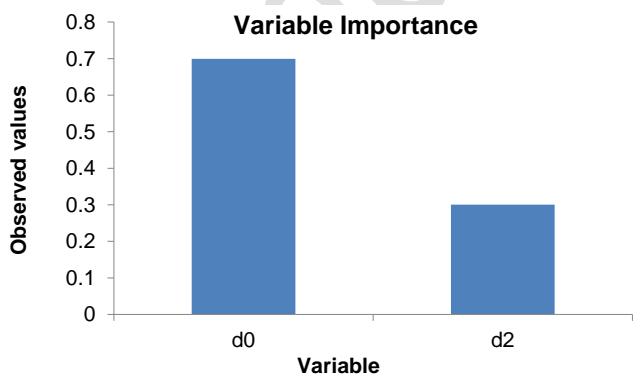
Fig. 2. Sensitivity analysis conducted in the GEP model.

**2.6. Climate data for future scenarios**

We utilized LARS-WG due to its superior performance and availability (Semenov *et al.*,1998). LARS-WG was employed to downscale GCM outputs for the Sangdeh station area, addressing the constraints of coarse-scale GCM data. To evaluate LARS-WG's performance, we reproduced observed daily data (rainfall, minimum and maximum temperature) from Sangdeh station (1 January 1985-31 December 2005) and generated 300 years of synthetic data. The statistical characteristics (mean and variance) of the observed data closely matched those of the synthetic data, demonstrating LARS-WG's effectiveness in generating observed data for the Kasilian Catchment. Using Sangdeh station's coordinates, LARS-WG created daily datasets for rainfall and temperature from all six models (ACCESS-ESM1-5, CNRM-CM6-1, GFDL-ESM4, HADGEM3-GC31-LL, MPI-ESM1-2-LR, MRI-ESM2-0) under one scenario (SSP585) for the periods (2031–2050 and 2051–2070). The SSP585 scenario is more suitable for modeling climate impacts in Iran because it aligns with the country's high fossil fuel consumption and slower renewable energy adoption. It projects more frequent and severe extreme weather events, which Iran is already experiencing. The scenario also provides a realistic assessment of future water scarcity, agricultural impacts, and shifts in biodiversity and ecosystems, making it crucial for planning and adaptation efforts in Iran. With climatic data (e.g., rainfall and temperature) for current and future conditions, the corresponding runoff can be determined for each condition to facilitate comparison. Typically, the runoff data for the future periods (2031-2050 and 2051-2070) should be compared with the runoff derived from the recorded data (2007-2018). Figs. 3 and 4 demonstrate improved model performance during the calibration period when integrating HEC-HMS with ANN and GEP models.

3. Results and discussion
3.1. Future Projections and Addressing Uncertainty from Diverse Climate Model Predictions

Different climate models yield diverse rainfall and runoff patterns (Semenov and Shewry, 2011). Studies in Iran show varying results: some models predict increased mean annual rainfall in northern Iran, while others forecast decreases in specific areas like Mazandaran in northern Iran (e.g., Abbaspour *et al.*, 2009; Babaeian *et al.*, 2007). Utilizing multiple climate models is crucial for precise climate change impact assessments. Two box plots were created using the future mean annual values of climatic variables (rainfall) and hydrological variables (runoff) from all General Circulation Models (GCMs) to illustrate the range of uncertainty in the predictions. These future values can be compared with historical data. The box plots display the 25th and 75th percentiles, the median (50th percentile), and the minimum and maximum values (Semenov and Shewry, 2011). Figs. 5 and 6 show annual changes in rainfall and runoff for two future periods.

During the calibration period from 2007 to 2018, the mean annual rainfall was 788 mm, while the mean annual runoff was 175.6 mm. Figs. 5 and 6 illustrate that the median (50th percentile) of mean annual rainfall from various climate models is projected to increase in the future under the SSP585 scenario compared to the base period (2007-2018). Conversely, the median (50th percentile) of mean annual runoff from these models is expected to decrease under the SSP585 scenario relative to the same base period. Rising temperatures and increased evapotranspiration are expected to reduce median annual runoff.
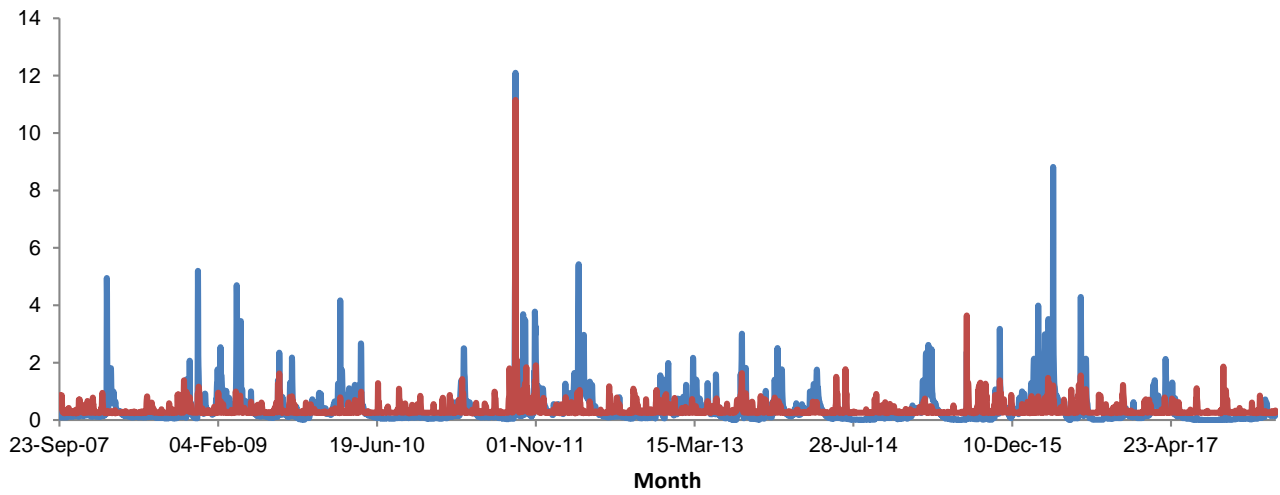
Fig. 3. The simulated (red) and observed (blue) hydrographs for the calibration period using Sangdeh rainfall station and integration of HEC HMS & ANN (3,3,1) models (with tansig activation function).
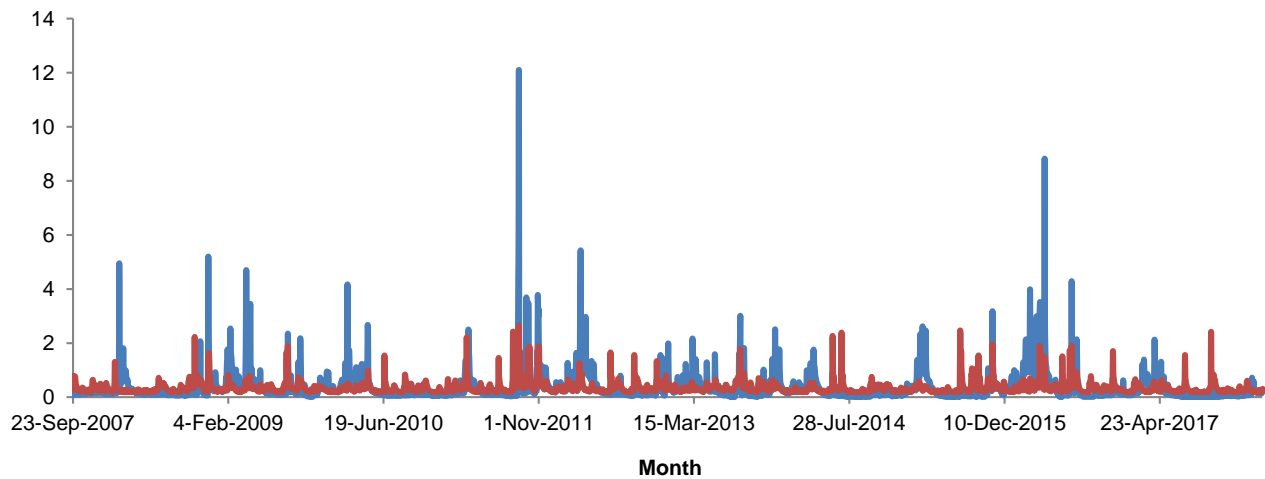

Fig. 4. The simulated (red) and observed (blue) hydrographs for the calibration period using Sangdeh rainfall station and integration of HEC HMS & GEP models.

Heavy rainfall is defined as daily precipitation amounts exceeding the 95th percentile of daily rainfall data for a specific period. For the observed period, the 95th percentile of wet days' precipitation was determined to be 25.81 mm/day. The frequency of wet days with heavy rainfall in the Kasilian Catchment was evaluated for the base period and two future periods under the SSP585 scenario (Fig. 7). During the observed period, there were 33 wet days with heavy rainfall. Projections indicate an increase in extreme precipitation events in future periods, as evidenced by the comparison of the median values in the boxplot and the number of wet days with heavy rainfall in the observed period.
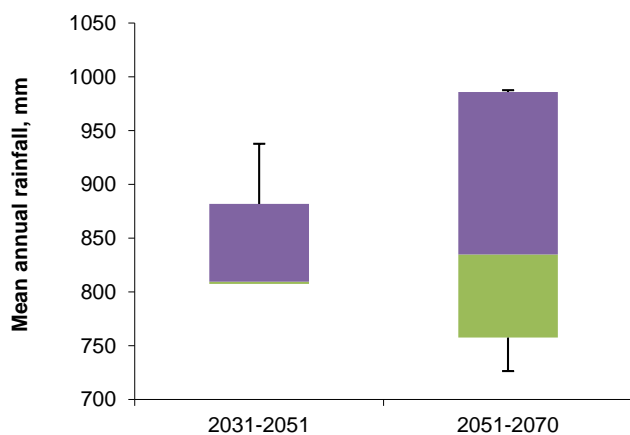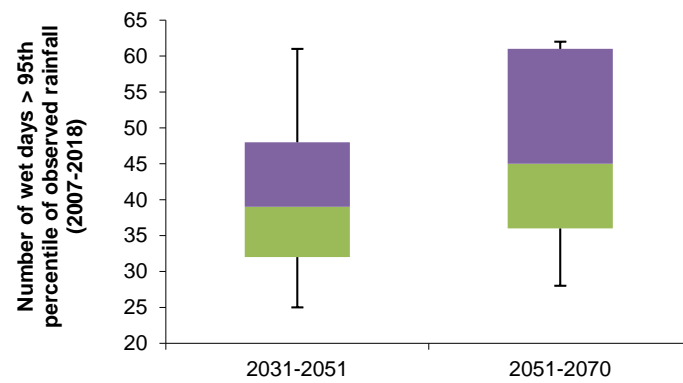

Fig. 5. Box plots constructed from the mean annual rainfall values obtained from different climate models for SSP585 scenario and future period.
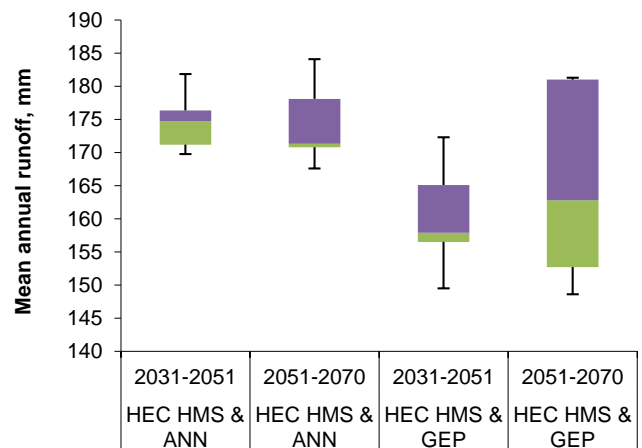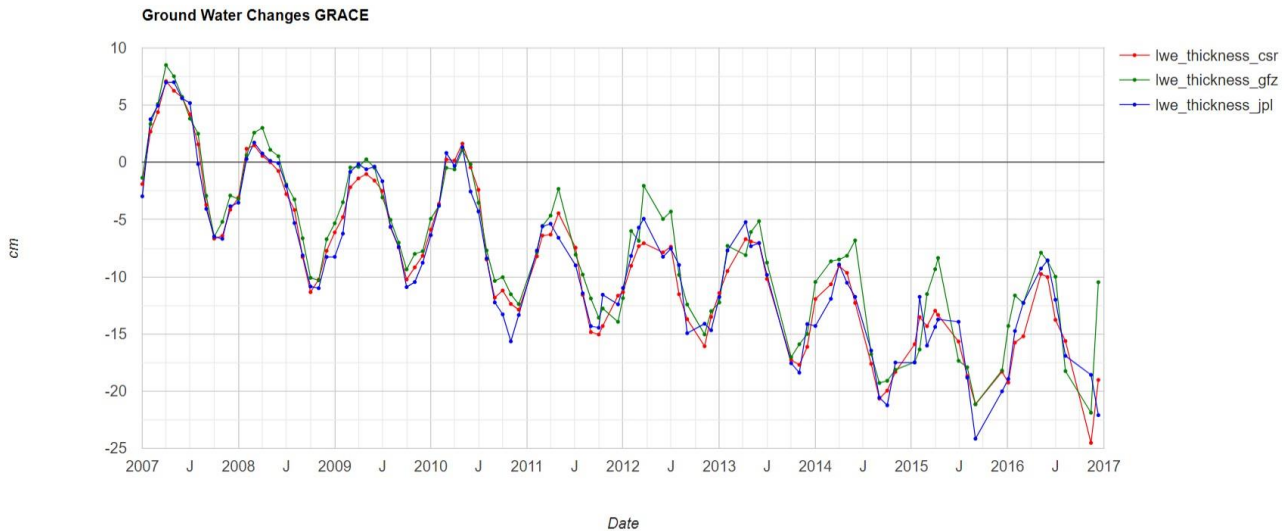

Fig. 6. Box plots constructed from the mean annual runoff values obtained from different climate models for SSP585 scenario and future period.

Fig. 7. Number of wet days for all future periods and climate models with precipitation > 95th percentile of the observed precipitation (2007–2018).

Fig. 8. Monthly Liquid Water Equivalent (LWE) thickness changes in the Kasilian Catchment from 2007 to 2016 Using GRACE and GEE Data.

Higher greenhouse gas levels may lead to more annual rainfall and extreme weather events (SWCS, 2003). Bae *et al.* (2008) projected an increase in mean annual rainfall for all catchments in South Korea for the period 2061-2090 compared to 1971-2000, but a decrease in mean annual runoff due to higher evapotranspiration. Shifteh Some'e *et al.* (2012) found that in Iran, annual rainfall increased by 0-10% from 1967 to 2006 in the northern regions. Rainfall in northern Iran is influenced by Siberian anticyclones. Weaker winter high-pressure systems have led to reduced winter rainfall, while stronger spring systems have increased spring rainfall, possibly leading to increased flooding in the southern Caspian Sea coastal region, where Kasilian is situated (Rasoli *et al.*, 2012).

Fig. 8, derived from Google Earth Engine (GEE) for the Kasilian Catchment, presents monthly Liquid Water Equivalent (LWE) thickness measurements from CSR, GFZ, JPL, and the GRACE satellite spanning January 2007 to December 2016. The data exhibits distinct seasonal patterns, with elevated LWE values in spring and summer and reduced values in fall and winter. Over the observed period, a general decline in LWE thickness is noted, particularly in the CSR and GFZ datasets. Despite variations in absolute values, the datasets display consistent trends. As Fig. 8 shows, currently, we are experiencing a decrease in underground water levels. In the future, increased mean rainfall, possibly due to more convective rainfall events, might lead to higher surface runoff and reduced groundwater infiltration. This is expected to significantly decrease the future decline in groundwater levels.

4. Conclusions

The GEP model outperformed the ANN and HEC-HMS models in modeling rainfall-runoff processes. However, both GEP and ANN models demonstrated similar accuracy in predicting runoff. By using the hybrid approach of incorporating streamflow series forecasts from conceptual models as inputs for ML models like ANN or GEP, it represents an advancement in hydrological modeling. This method not only improves the accuracy of runoff predictions but also proves highly useful for assessing the effects of climate change on water resources, particularly runoff. Climate change in the Kasilian Catchment and northern Iran could lead to more extreme rainfall events and an increase in mean annual rainfall. However, higher evapotranspiration may result in decreased annual runoff. The rise in mean rainfall might be driven by these extreme events, potentially causing more flooding and erosion in smaller catchments and reducing groundwater recharge in northern Iran. To mitigate flooding, erosion, and enhance groundwater recharge in mountainous forested areas experiencing deforestation, such as the Kasilian catchment near the catchment's outlet, strategies include reforestation to stabilize soil and absorb rainfall, wetland restoration to act as natural water filters and flood buffers, and establishing riparian buffers along waterways. Improved agricultural practices like contour farming, cover crops, and terracing can reduce runoff, while water management techniques such as rainwater harvesting, infiltration basins, and check dams help managing stormwater. Soil conservation measures like mulching and no-till farming further reduce erosion. Engaging local communities through awareness programs and participatory planning ensures successful implementation.

Author Contributions

The corresponding author handled all tasks, including writing, calculations, and data collection. The second author, an expert in computer engineering, provided support specifically for the computer-related sections of the paper and developed the ANN implementation.

Conflict of Interest

The authors declare no competing interests and non-financial competing interests.

Acknowledgments

Data Availability Statement

The datasets used and/or analyzed during the current study are available from the corresponding author on reasonable request.

References

Abbaspour, K.C. *et al.* (2009) 'Assessing the impact of climate change on water resources in Iran', *Water Resources Research*, 45(10), p. W10434. doi: https://doi.org/10.1029/2008WR007615

Asadi, H., and Santos, C.A.G. (2022) 'A hybrid artificial intelligence and semi-distributed model for runoff prediction', *Water Supply*, 22(7), pp. 6181-6195. doi: https://doi.org/10.2166/ws.2022.123

Aytek, A., Asce, M., and Alp, M. (2008) 'An application of artificial intelligence for rainfall-runoff modeling', *Journal of Earth System Science*, 117, pp. 145–155. doi: https://doi.org/10.1007/s12040-008-0005-2

Azamathulla, H.M. (2012) 'Comment on "Reverse level pool routing: comparison between a deterministic and a stochastic approach" by Marco D'Oria, Paolo Mignosa, Maria Giovanna Tanda', *Journal of Hydrology*, 470-471, p. 328. doi: https://doi.org/10.1016/j.jhydrol.2012.07.045

Babaeian, I. *et al.* (2007) 'Climate change investigation of Iran for 2010-2039 using downscaled output of ECHO-G climate model', *Geography and Development Iranian Journal*, 16, pp. 135-152 (in Persian). doi: https://doi.org/10.22111/gdij.2009.1179

Bae, D.H., Jung, W., and Chang, H. (2008) 'Potential changes in Korean water resources estimated by high-resolution climate resolution', *Climate Research*, 35, pp. 213-226. doi: https://doi.org/10.3354/cr00704

Bae, D.H., Jung, W., and Lettenmaier, D.P. (2011) 'Hydrologic uncertainties in climate change from IPCC AR4 GCM simulations of the Chungju Catchment, Korea', *Journal of Hydrology*, 401, pp. 90–105. doi: https://doi.org/10.1016/j.jhydrol.2011.02.012

Bakhshaei, M. *et al.* (2021) 'Runoff estimation in urban catchment using Artificial neural network models', *Plant Archives*, 21(S1), pp. 2253-2260. doi: https://doi.org/10.51470/PLANTARCHIVES.2021.v21.S1.371

Chavoshi, S. *et al.* (2013) 'Flood prediction in southern strip of Caspian Sea watershed', Water Resources, 40(6), pp. 593-605. doi: https://doi.org/10.1134/S0097807813060122

Farfán, J.F. *et al.* (2020) 'A hybrid neural network-based technique to improve the flow forecasting of physical and data-driven models: methodology and case studies in Andean watersheds', *Journal of Hydrology Regional Studies*, 27, p. 100652. doi: https://doi.org/10.1016/j.ejrh.2019.100652

Ferreira, C. (2006). 'Gene expression programming: mathematical modeling by an artificial intelligence', (Vol. 21). Springer. doi: https://doi.org/10.1007/3-540-32849-1

Gebremichael, M., and Hailu, A. (2024) 'Comparative analysis of HEC-HMS and machine learning models for rainfall-runoff prediction', *Hydrology Research*, 55(3), pp. 456-470. doi: https://doi.org/10.2166/nh.2024.032

Hajian, F. (2013) Effects of land cover and climate changes on runoff and sediment yield from a forested catchment in northern Iran. PhD thesis. Kingston University.

Hitokoto, M., and Sakuraba, M. (2020) 'Hybrid deep neural network and distributed rainfall-runoff model for real-time river-stage prediction', *Journal of Japan Society of Civil Engineers (JSCE)*, 8(1), pp. 46–58. doi: https://doi.org/10.2208/journalofjsce.8.1_46

Kisi, O., Shiri, J., and Tombul, M. (2013) 'Modeling rainfall-runoff process using soft computing techniques', *Computers & Geosciences*, 51, pp. 108–117. doi: https://doi.org/10.1016/j.cageo.2012.07.001

Motamednia, M., Nohegar, A., Malekian, A., Asadi, H., Tavasoli, A., Safari, M. and Karimi Zarchi, K. (2015) 'Daily river flow forecasting in a semi-arid region using two data driven', Desert, 20(1), pp. 11-21.

Ömer Faruk, A., and Ayan, K. (2015) 'Software defect prediction using cost-sensitive neural network', *Applied Soft Computing*, 33, pp. 263-277. doi: https://doi.org/10.1016/j.asoc.2015.04.045

Pashazadeh, A., and Javan, M. (2019) 'Comparison of the gene expression programming, artificial neural network (ANN), and equivalent Muskingum inflow models in the flood routing of multiple branched rivers', *Theoretical and Applied Climatology*, doi: https://doi.org/10.1007/s00704-019-03032-2

Pashazadeh, A., and Javan, M. (2020) 'Comparison of the gene expression programming, artificial neural network (ANN), and equivalent Muskingum inflow models in the flood routing of multiple branched rivers', *Theoretical and Applied Climatology*, 139(3), pp. 1349-1362. doi: https://doi.org/10.1007/s00704-019-03032-2

Rasoli, A. *et al.* (2012) 'Time series analysis of pressure of centre of synoptic patterns influencing the seasonal rainfall of Iran', *Geography and Development*, 27, pp.77-88.

Romański, L. *et al.* (2017) 'Estimation of operational parameters of the counter-rotating wind turbine with artificial neural networks', *Archives of Civil and Mechanical Engineering*, 17(4), pp. 1019-1028. doi: https://doi.org/10.1016/j.acme.2017.04.010

Scharffenberg, W.A. and Fleming, M.J. (2010) 'Hydrologic Modelling System HEC-HMS User's Manual', US Army Corps of Engineers, Hydrologic Engineering Center.

Semenov, M., and Shewry, P.R. (2011) 'Modelling predicts that heat stress, not drought, will increase vulnerability of wheat in Europe', *Scientific Reports*, 1, p. 66. doi: https://doi.org/10.1038/srep00066

Semenov, M.A. *et al.* (1998) 'Comparison of the WGEN and LARS-WG stochastic weather generators for diverse climates', *Climate Research*, 10, pp. 95–107. doi: https://doi.org/10.3354/cr010095

Shifteh Some'e, B., Ezani, A., and Tabari, H. (2012) 'Spatiotemporal trends and change point of precipitation in Iran', Atmospheric Research, 113, pp. 1-12. doi: https://doi.org/10.1016/j.atmosres.2012.04.016

Shiri, J. *et al.* (2012) 'Forecasting daily stream flows using artificial intelligence approaches', *ISH Journal of Hydraulic Engineering*, 18(3), pp. 204–214. doi: https://doi.org/10.1080/09715010.2012.721189

SWCS (2003) Conservation implications of climate change: soil erosion and runoff from cropland. A Report from the Soil and Water Conservation Society. Ankeny, Iowa: Soil and Water Conservation Society. Available at: https://www.swcs.org/docs/climate%20change-final.pdf (Accessed: 1 November 2024).

Valipour, M., Banihabib, M.E., and Behbahani, S.M.R. (2013) 'Comparison of the ARMA, ARIMA, and the autoregressive artificial neural network models in forecasting the monthly inflow of Dez dam reservoir', *Journal of Hydrology*, 476, pp. 433–441. doi: https://doi.org/10.1016/j.jhydrol.2012.11.017

Wang, W-C. *et al.* (2009) 'A comparison of performance of several artificial intelligence methods for forecasting monthly discharge time series', *Journal of Hydrology*, 374, pp. 294–306. doi: https://doi.org/10.1016/j.jhydrol.2009.06.019